


RESEARCH ARTICLE OPEN ACCESS

Organocatalytic Acetalization of Aldehydes Utilizing N-Heterocyclic Iod(az)olium Salts as the Halogen-Bonding Catalysts

Eirini M. Galathri¹ | Kostas Tsampalis^{1,2} | Thomas J. Kuczmera³ | Demeter Tzeli^{4,5} | Boris J. Nachtsheim³ | Christoforos G. Kokotos¹ 

¹Laboratory of Organic Chemistry, Department of Chemistry, National and Kapodistrian University of Athens, Athens, Greece | ²Pnoilab SA, Gerakas, Greece |

³Institute For Organic and Analytical Chemistry, University of Bremen, Bremen, Germany | ⁴Laboratory of Physical Chemistry, Department of Chemistry, National and Kapodistrian University of Athens, Athens, Greece | ⁵Theoretical and Physical Chemistry Institute, National Hellenic Research Foundation, Athens, Greece

Correspondence: Christoforos G. Kokotos (ckokotos@chem.uoa.gr)

Received: 14 October 2025 | **Revised:** 28 November 2025 | **Accepted:** 15 December 2025

Keywords: acetalization | halogen bond | heterocyclic iod(az)olium salts | organocatalysis

ABSTRACT

The formation of acetals from aldehydes is a valuable transformation in organic synthesis and biological systems. In this study, complementing experimental screening and density functional theory (DFT) calculations were performed to predict the relative effectiveness of five potential halogen-bonding (XB) catalysts for the acetalization reaction between 3-phenylpropanal and methanol. By analyzing electrostatic potential maps, I...O distances, binding energies, and Gibbs free energy changes, the computational study provided a theoretical ranking to guide and rationalize catalyst selection, highlighting the synergy between experimental and computational approaches in catalyst development. We report a mild, cost-effective, and organocatalytic protocol employing iod(az)olium salts as XB catalysts to promote the acetalization of various aliphatic and aromatic aldehydes, achieving good yields.

1 | Introduction

Aldehydes are highly important moieties in organic synthesis, due to their reactive nature, although their high reactivity can sometimes hinder desired transformations [1–4]. To address this issue, converting carbonyl groups into acetals is a widely used protection method, particularly in pharmaceutical industry and drug design [5–7]. Acetals serve as effective protecting groups, due to their stability under neutral or basic conditions, allowing for a range of reactions. Additionally, acetals have been identified as valuable intermediates in synthetic chemistry [8–13] and are used as flavoring agents, aroma enhancers in

cosmetics and food products [14] and as anti-freezing additives in biodiesel [15].

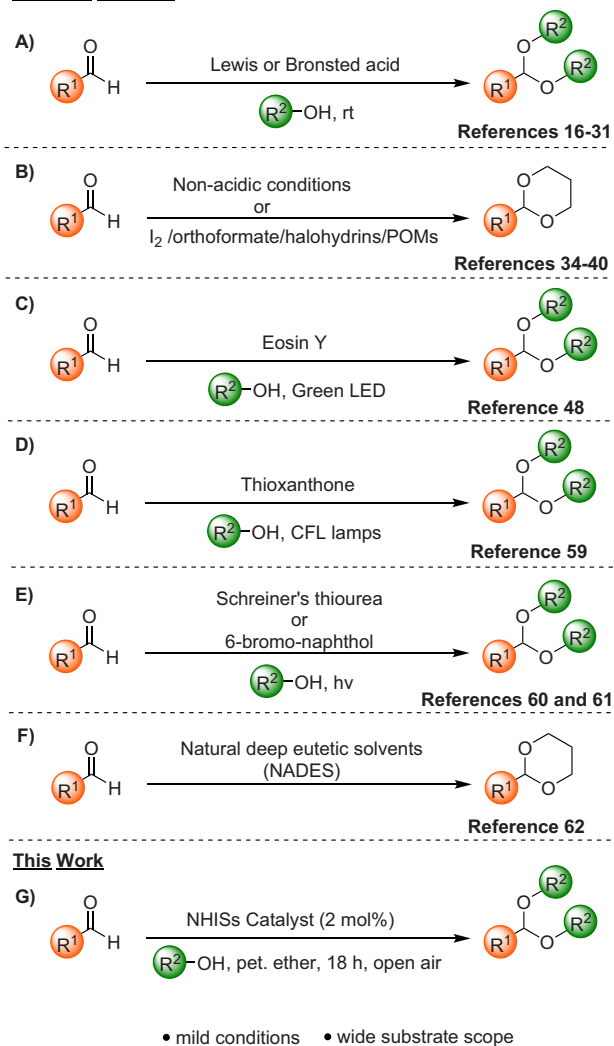
Numerous methodologies have been developed for the conversion of aldehydes into acetals to protect them against oxidation and undesired nucleophilic attack. Traditional acetalization approaches often involve strong mineral acids, like HCl [16–18], solid acids [19], acidic polymers [20, 21], metal catalysts [22–29], or Lewis and organic acids [30, 31] (Scheme 1a). However, these methods are associated with significant drawbacks, including corrosive conditions, extended reaction times, and often poor selectivity, which raise environmental concerns [32]. To address

Eirini M. Galathri and Kostas Tsampalis contributed equally to this study.

This is an open access article under the terms of the [Creative Commons Attribution](https://creativecommons.org/licenses/by/4.0/) License, which permits use, distribution and reproduction in any medium, provided the original work is properly cited.

© 2026 The Author(s). *ChemCatChem* published by Wiley-VCH GmbH

Previous Methods



SCHEME 1 | Common synthetic pathways for the acetalization of aldehydes (A-F) and this work (G).

these issues and align with green and sustainable chemistry principles [33], alternative methods for acetal synthesis have been explored. Acetalization of carbonyl compounds can also be achieved under basic [34] or nonacidic conditions, using reagents, such as hydroxylamine [35], iodine [36, 37], trialkyl orthoformates [38], halohydrins [39], or catalytic amounts of anionic metal oxides, like polyoxometalates (POMs) [40] (Scheme 1b).

Nowadays, organic synthetic photochemistry has emerged as an alternative methodology to produce highly interesting compounds [41–47]. In 2017, an innovative photochemical approach was introduced, utilizing Eosin Y as the photocatalyst and green LED irradiation, achieving excellent yields in aldehyde acetalization (Scheme 1c) [48]. However, the authors did not clarify whether the acidic groups on Eosin Y or the heat emitted by the green LED contributed to or were the primary driving force of the reaction's success. Our laboratory is active for many years in the field of photochemistry, utilizing a variety of photocatalysts and study the reaction mechanism of various photochemical reactions [49–58]. In 2019, the Kokotos group developed a novel photochemical approach for the acetalization of aldehydes with alcohols or diols, utilizing thioxanthone as the catalyst and

household lamps as the light source (Scheme 1d) [59], whereas in 2020, we presented a novel, mild and green photochemical protocol for the synthesis of acetals from aldehydes, utilizing Schreiner's thiourea as the photoacid and household lamps as the irradiation source [60]. In 2022, another photoacid-catalyzed acetalization was demonstrated by Badillo and coworkers, utilizing 6-bromo-2-naphthol as the catalyst (Scheme 1e) [61], whereas Prandi and coworkers, in 2023, reported the synthesis of acetals in acidic natural deep eutectic solvents (NADES) [62]. In that protocol, the solvent participates itself in the catalytic promotion of the reaction and the reaction medium is completely recycled and reused without any loss of catalytic activity even after ten consecutive cycles (Scheme 1f) [62].

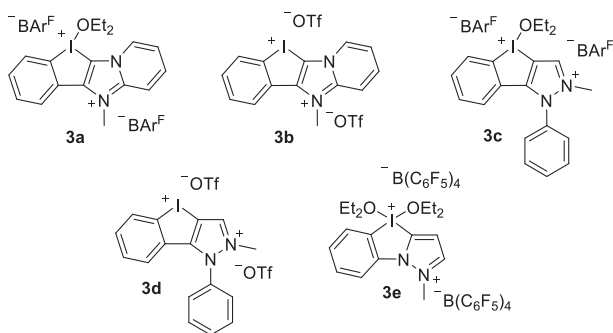
Halogen-bonding (XB), which involves the interaction between electrophilic halogen atoms and Lewis bases (LBs), has been extensively investigated over the past two decades [63–65]. This interaction has found successful applications in various fields, including crystal engineering [66], anion recognition [67], organic synthesis [67], and organocatalysis [68]. In recent years, XB catalysis has gained significant interest, due to growing concerns regarding the use of metal catalysts [69–75]. Among XB catalysts, those based on iodine have played a leading role. These catalysts are increasingly recognized for their affordability, stability, environmental friendliness and ease in handling [76, 77], contributing to their growing relevance in organocatalysis. The field gained momentum in 2008, when Bolm and colleagues reported the use of perfluoroiodoalkanes as XB catalysts [78].

Developing new catalysts for organic transformations typically requires extensive experimental screening, making the process both time-consuming and resource-intensive. The acetalization of 3-phenylpropanal with methanol serves as a representative reaction, where catalyst choice greatly affects efficiency and selectivity. To streamline catalyst discovery, computational studies can provide predictive insights into catalytic performance prior to experimental validation. The aim of our computational study was to deliver theoretical guidance for prioritizing catalysts with high predicted activity, thereby reducing experimental workload and enhancing mechanistic understanding. By integrating computational predictions with experimental validation, this approach exemplifies a modern, efficient strategy for catalyst development and optimization.

The research group of Nachtsheim has investigated in detail the application of N-heterocyclic iod(az)olium salts (NHISs) as XB catalysts [79–85]. In a previous collaborative effort, we employed XB to facilitate the reaction between aldehydes and indole, leading to the synthesis of biologically and pharmaceutically relevant bis(indolyl)methanes (BIMs) [75]. In this study, we present a novel, mild and inexpensive method for the acetalization of aldehydes with alcohols or diols, utilizing NHISs as XB catalysts (Scheme 1g).

2 | Results and Discussion

Initially, five XB compounds, **3a–3e** (Scheme 2), were calculated via density functional theory (DFT) calculations to investigate their potential to be used as organocatalysts. Given that there are many possible conformers for each molecular system, a con-



SCHEME 2 | Chemical structures of compounds **3a–3e**.

former search was performed using the CREST 3.0 tool developed by Grimme [86, 87], when the molecular system was comprised of only one molecule, or the DOCKER algorithm of Orca 6.0 package [88–93], when the system was comprised of more than one molecules (see [Supporting Information](#)). Then, for the five lowest in energy structures of each molecular system, their geometries were optimized via DFT calculations at the B3LYP [94–97]/def2-SVP [98, 99] method in methanol as the solvent, using the SMD solvation model. Then, the lowest in energy molecular structures were further optimized at the wB97X-D4 [100, 101]/def2-TZVP [99], where the Grimme's D4 atomic-charge dependent London dispersion correction has been included [94, 102, 103].

The importance of the inclusion of dispersion correction is presented in the [Supporting Information](#). Finally, a single point energy calculation was carried out at wB97X-D4/def2-TZVPP//wB97X-D4/def2-TZVP along with the DRACO [104] solvation model to provide extra accuracy, compared to the standard SMD model [105]. Furthermore, frequencies were calculated at the wB97X-D4/def2-TZVP method to verify that the calculated molecular systems are true minimum structures. Moreover, all energies were corrected with respect to the basis set superposition error (BSSE) [106]. Finally, the electrostatic potential of the initial reactant and XB donor catalysts were calculated on the 0.001 a.u. isosurfaces of the electron density using the MultiWFN program [107] and were visualized using the UCSF ChimeraX program [108].

Electrostatic surface potential (ESP) calculations were performed to evaluate the electronic environments of the reactant 3-phenylpropanal (**1a**) and the potential iodine-containing catalysts **3a–3e** as ESP plays an important role in understanding XB [109–111]. The ESP minimum ($V_{s,\min}$) and maximum ($V_{s,\max}$) values provide insights into the regions of negative and positive electrostatic potential, respectively, which are directly related to potential nucleophilic and electrophilic reactivity. The electrostatic potential maps of the initial reactant **1a** and the iodine catalysts (**3a–3e**) were calculated (Figure 1). For aldehyde **1a**, the $V_{s,\min}$ of -46.2 kcal/mol is consistent with the electron-rich oxygen of the aldehyde group, whereas the $V_{s,\max}$ of 32.5 kcal/mol corresponds to the partial positive charge at the carbonyl carbon, the site of nucleophilic attack. The ESP analysis for the iodine-containing molecules shows that the area surrounding iodine holds the most positive (blue) values, creating “ σ -hole” regions along the C–I axis. Therefore, the non-covalent halogen bond can

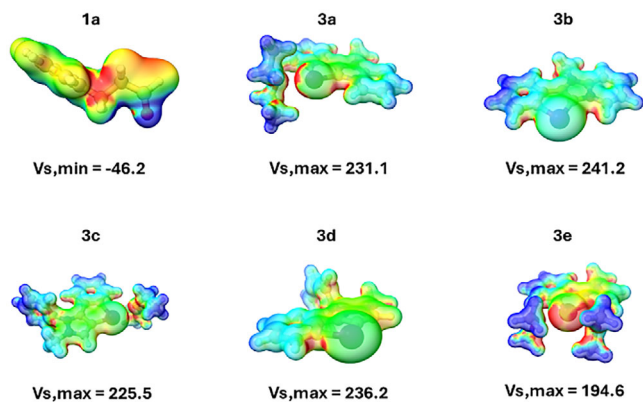


FIGURE 1 | Electrostatic potential maps on the 0.001 a.u. contour of the electronic density for 3-phenylpropanal (**1a**), **3a**, **3b**, **3c**, **3d**, and **3e**, in map are blue (positive) and red (negative) in kcal/mol. The range for **1a** is $-46.2 + 32.5$, whereas for **3a–3e** is $+93.9 + 241.2$, corresponding to the minima and maxima for each compound.

be formed by the oxygen atom of the aldehyde interacting with the iodine atom of the catalysts. $V_{s,\min}$ and $V_{s,\max}$ values, presented in Table 1 are among the factors influencing each catalyst's potential to improve reaction yield. Catalysts will participate in a non-covalent halogen bond between the iodine and the oxygen of the aldehyde, meaning that the $V_{s,\min}$ area of the aldehyde will interact with the $V_{s,\max}$ area of the catalysts. It would make sense that the higher the maximum potential of the catalyst, the more efficient this interaction would be, taking of course into account the steric hindrances that result from the catalysts topology at the area around iodine. Although $V_{s,\max}$ is a deciding factor of the catalysts' inherent electrophilicity, the difference (drop) in $V_{s,\max}$ is also of great importance, as it indicates a higher “charge transfer” character during the halogen bond formation. The expected mechanism of catalysis is a σ -hole interaction, driven by $V_{s,\max}$ of the catalyst, but a bigger drop in V would indicate a higher charge transfer and stronger binding, factors that would “poison” the catalyst and lower yield. Indeed, as per the results in Table 1, even though **3b** has the highest $V_{s,\max}$ with **3d** coming second, after binding, the complexes exhibit a different behavior with **3d** having the greatest value (only a -11.5 kcal/mol drop) and **3b** dropping to third place (-45.3 kcal/mol) even after **3e** (-5.5 kcal/mol). In addition to the ESP values, the polarizability and magnetic shielding of the iodine were calculated and especially their change upon complexation of the catalyst with the reactant. The change in anisotropy suggests that the more potent the catalyst is, the lower the change should be (negative in some cases), whereas the catalysts that showcase high steric hindrances result in a more distorted electron cloud (higher Δ values, see [Supporting Information](#) for extended data presentation).

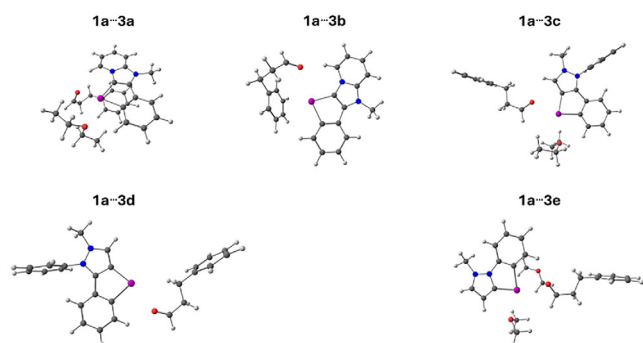
After examining the ESP of each component, we proceeded to the calculation of complexes' (pre-reaction complexes) geometrical properties, mainly the I...O distance and the C...I...O angle, which are the most representative factors when studying the non-covalent halogen bond interaction. As seen in Table 2, all I...O distances fall within the typical non-covalent bond distance range of $2.5\text{--}3.3$ Å, but spatial variation is observed, with **1a-3c**, **1a-3d**, and **1a-3e** complexes being closer to the standard 2.55 Å typical distance, whereas **1a-3a** and **1a-3b** have a prolonged I–O distance

TABLE 1 | Electrostatic potential (V_s) minimum and maximum values for 3-phenylpropanal (**1a**), **3a**, **3b**, **3c**, **3d**, and **3e**.

Entries	Species	$V_{s,\min}$ (kcal/mol)	$V_{s,\max}$ (kcal/mol)	Complex—monomer $\Delta V_{s,\max}$ (kcal/mol)
1	1a	-46.2	32.5	-
2	3a	96.7	231.1	-36.0
3	3b	112.8	241.2	-45.3
4	3c	93.9	225.5	-43.5
5	3d	99.4	236.2	-11.5
6	3e	112.8	194.6	-5.5

TABLE 2 | Calculated I...O distance in Å for the various complexes of 3-phenylpropanal (**1a**) with **3a**, **3b**, **3c**, **3d**, or **3e**.

Entries	Complexes	I...O distance (Å)	C...I...O angle (°)
1	1a-3a	3.166	155.26
2	1a-3b	3.026	172.26
3	1a-3c	2.789	157.03
4	1a-3d	2.867	168.27
5	1a-3e	2.721	164.87

**FIGURE 2** | Optimized geometries of the reactant **1a** and the reactant's complexes with the catalysts (**3a-3e**).

of >3.0 Å. Similar observations can be made about the C...I...O angle, which greatly influences the interaction between the active sites, as the C-I axis is where the σ -hole region is present. Again, **1a-3b** and **1a-3d** show the most geometrically favorable approach of the aldehyde's oxygen to the C-I axis, followed closely by **1a-3e**, whereas in the cases of **1a-3a** or **1a-3c**, the oxygen approaches at a lower angle of $>10^\circ$ – 15° , due to the steric hindrances presented by the catalysts' OEt₂ group oxygen (Figure 2).

Finally, to further assess the strength of non-covalent interactions between **1a** and the iodine-containing molecules **3a-3e**, binding energies (ΔE) were computed using the counterpoise-corrected Boys and Bernardi formula [106]. This approach effectively accounts for basis set superposition error (BSSE), ensuring accurate estimation of interaction strengths. The calculated binding energies range from -7.0 to 11.3 kcal/mol as shown in Table 3, indicating moderate to strong non-covalent association between the aldehyde and the potential catalysts. Among the systems studied, complex **1a-3a** exhibits the most favorable binding energy

(11.3 kcal/mol), suggesting a particularly stable pre-reaction complex. Complexes **1a-3b** (8.7 kcal/mol) and **1a-3c** (7.9 kcal/mol) also demonstrate strong association with the aldehyde, indicating efficient non-covalent stabilization in the pre-reactive state. In contrast, **1a-3d** displays the weakest interaction (7.0 kcal/mol), suggesting weaker complexation under the same conditions. Additionally, all ΔH_{bind} values were also negative and range from -8.6 to -3.8 kcal/mol, concluding to the fact that the generation of the complexes is an exothermic process, whereas ΔG_{bind} values are positive at 298.15K , due to the decrease of entropy and the most exoenergetic ΔG_{bind} values are obtained for entry 5 (**1a-3e**), at 11.5 kcal/mol. Overall, the data of Table 3 suggest that all aldehyde-catalyst complexes may be in rapid dynamic equilibrium with their components at room temperature.

This computational study assessed the catalytic potential of iodine (III)-based halogen bond donor catalysts **3a-3e** in the acetalization of **1a**. Using a combination of electrostatic potential analysis, optimized reactant-catalyst complex geometries and binding energies, we identified key factors influencing catalytic activity (Table 4). To evaluate the potential catalytic efficiency of each candidate, a qualitative multiparameter scoring protocol was developed to rank all catalysts (Table 5). The scores range from 0 (least favorable) to 1 (most favorable) and are normalized relative to the variation of values within the dataset for each parameter. The selection of these specific criteria is grounded in the fundamental physical requirements of XB catalysis which are as follows: Electrostatics—a higher $V_{s,\max}$ is favorable, as it corresponds to a deeper σ -hole capable of stronger electrophilic activation of the aldehyde's carbonyl oxygen. Geometry (distance and angle)—a shorter I...O distance is preferred, indicating a tighter pre-reaction association. Furthermore, a C-I...O angle closer to 180° is favorable, as XB is highly directional and linearity is required for optimal orbital overlap ($n \rightarrow \sigma^*$). Thermodynamics—a higher binding energy score (representing

TABLE 3 | Binding energies (ΔE_{bind}), binding enthalpies, and binding Gibbs free energies (ΔG_{bind}) for each aldehyde-catalyst complex.

Entries	Complexes	ΔE_{bind} (kcal/mol)	ΔH_{bind} (kcal/mol)	ΔG_{bind} (kcal/mol)
1	1a-3a	-11.3	-8.6	6.6
2	1a-3b	-8.7	-4.8	8.1
3	1a-3c	-7.9	-4.9	9.2
4	1a-3d	-7.0	-3.8	10.2
5	1a-3e	-7.1	-4.2	11.5

TABLE 4 | Complete data table for catalysts **3a-3e**.

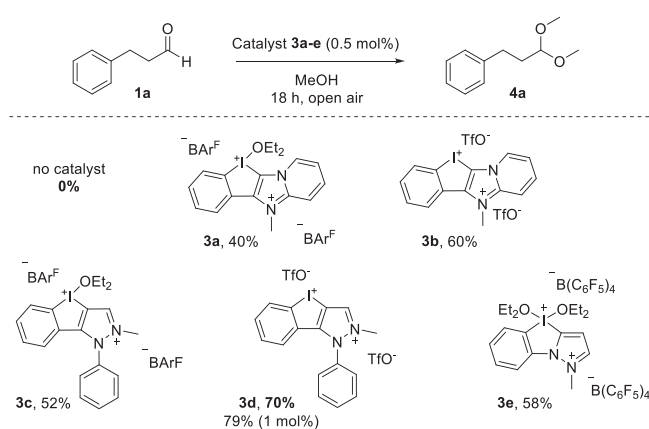
Species	$V_{s, \text{min}}$ (kcal/mol)	$V_{s, \text{max}}$ (kcal/mol)	I...O distance (Å)	C...I...O angle (°)	Binding E (kcal/mol)
3a	96.7	231.1	3.166	155.26	-11.3
3b	112.8	241.2	3.026	172.26	-8.7
3c	93.9	225.5	2.789	157.03	-7.9
3d	99.4	236.2	2.867	168.27	-7.0
3e	112.8	194.6	2.721	164.87	-7.1

TABLE 5 | Final scores for catalysts **3a-3e**.

Species	Score average	Score ($V_{s, \text{max}}$)	Score I...O distance	Score C...I...O angle	Score binding energy
3d	0.83	0.89	0.67	0.77	1.00
3b	0.73	1.00	0.32	1.00	0.62
3e	0.64	0.00	1.00	0.57	0.98
3c	0.60	0.66	0.85	0.10	0.80
3a	0.20	0.78	0.00	0.00	0.00

moderate binding) is favorable, reflecting the Sabatier principle; an overly strong binding interaction (low energy value) could prevent product release, leading to catalyst poisoning. The resulting average scores, presented in Table 5, are sorted in descending order. The necessity of this multiparameter approach is evident, when analyzing catalyst **3b**. Relying solely on the electrostatic potential would predict **3b** ($V_{s, \text{max}} = 241.2$ kcal/mol) as the superior catalyst. However, the scoring system correctly penalizes **3b** for its unfavorable geometric parameters (prolonged I...O distance due to steric hindrance), thereby identifying **3d** as the more balanced, effective candidate. The final classification of catalytic potency is **3d** > **3b** > **3e** > **3c** > **3a**. It should be noted that while a direct linear correlation between the calculated score and experimental yield is not observed, due to the multifactorial nature of the reaction, the system successfully predicts the rank order of catalytic efficiency. This confirms its utility as a qualitative screening tool to prioritize 'Goldilocks' [112, 113] candidates (like **3d**) and filter out low-potency catalysts (like **3a**) prior to experimental synthesis.

Following these extensive computational studies, we began our investigations by studying the acetalization of 3-phenylpropanal (**1a**) with methanol as both reagent and solvent at room temperature to form (3,3-dimethoxypropyl)benzene (**4a**) (Scheme 3).

**SCHEME 3** | N-Heterocyclic iod(az)olium salts (NHISs) as catalysts for the acetalization of 3-phenylpropanal (**1a**) with methanol. BArF^- : tetrakis[3,5-bis(trifluoromethyl)phenyl]borate.

The absence of catalyst did not lead to product formation. Then, we screened **3a-3e** as the potential XB catalysts [85]. Among the compounds tested, catalyst **3d** afforded the highest yield (70%), when employed in a very low catalyst loading (0.5 mol%, Scheme 3). However, upon increasing the catalyst

TABLE 6 | Solvent screening for the synthesis of acetal **4a** from aldehyde **1a**.

Entries	Solvent	Yield ^a (%)
1	MeCN	63
2	CH ₂ Cl ₂	70
3	CHCl ₃	78
4^b	CHCl ₃	81
5	EtOAc	68
6	DMSO	20
7	Toluene	69
8	Pet. Eth.	65
9^b	Pet. Eth.	85
10	THF	34
11	H ₂ O	32
12	Et ₂ O	43
13	2-Me-THF	25

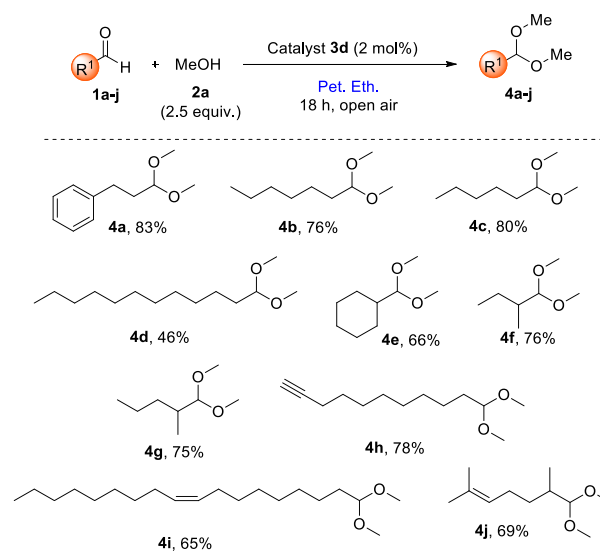
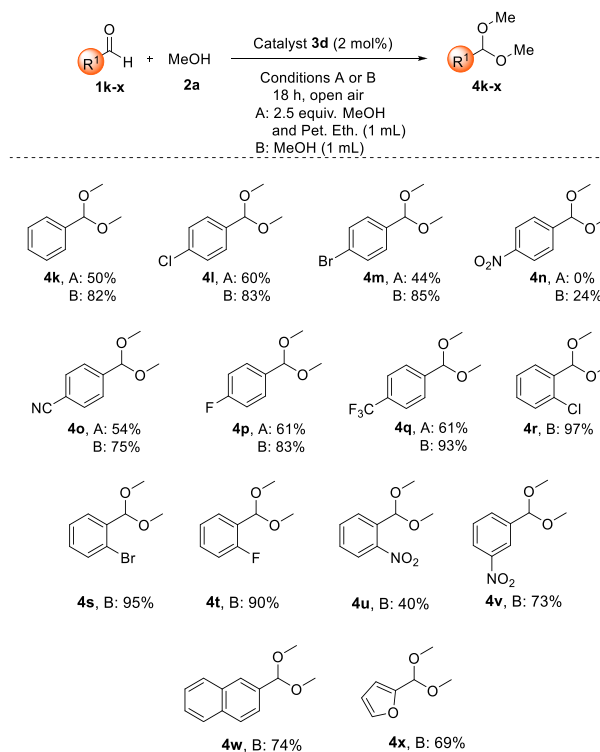
^aYield determined by ¹H-NMR using 1,3,5-trimethoxybenzene as internal standard. The reaction was performed with 3-phenylpropanal (**1a**) (67 mg, 0.50 mmol), methanol (40 mg, 1.25 mmol), and catalyst **3d** (1 mol%, 5.0 μmol) in solvent (1 mL) for 18 h.

^bYield determined by ¹H-NMR using internal standard with 2 mol% catalyst **3d**.

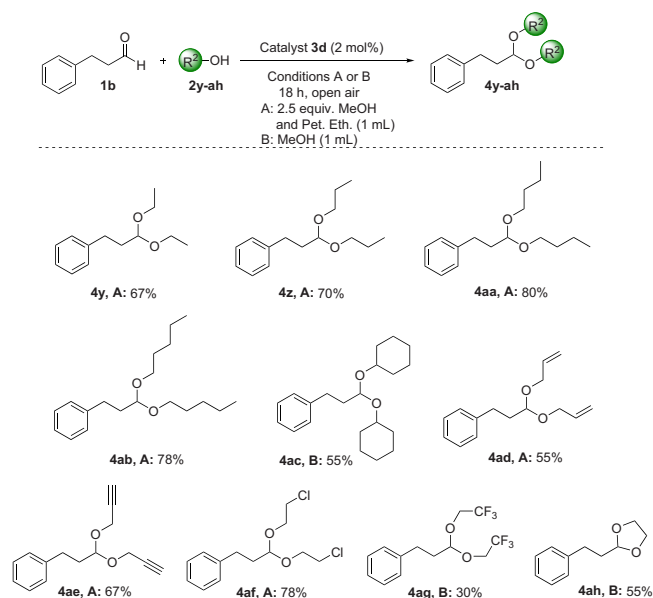
loading to 1 mol%, the desired product was isolated in 79% yield. As shown by the experimental yields, alongside the calculated studies, catalysts **3d** and **3b** indeed exhibit the highest catalytic efficiencies, while **3a** is the least effective. Catalysts **3c** and **3e** demonstrate intermediate performance. Although a straightforward linear correlation between calculated and experimental data is not evident, this study demonstrates that the relative catalytic potency can be reliably and qualitatively predicted by evaluating key energetic and geometric parameters across the catalyst series. While the intermediate catalysts (**3c** and **3e**) cannot be distinctly separated in terms of performance based solely on these descriptors, the extremes of the catalytic activity range—the most and least effective catalysts—are well predicted by the computational metrics.

Next, we screened a number of common solvents by running the acetalization reaction of **1a** with MeOH (**2a**) (2.5 equiv.) (Table 6). Chloroform and petroleum ether afforded the highest yields (78% and 65%, respectively). However, when we increased the catalytic loading from 1 to 2 mol% for these two optimal solvents, petroleum ether led to the highest yield (85%) (Table 6, entry 9).

Having in hand the optimum reaction conditions utilizing N-heterocyclic iod(az)olium salt **3d** as the XB catalyst and petroleum ether as the solvent, we turned our attention to exploring the substrate scope (Schemes 4–6). First, we explored the scope of the aldehydes with methanol. A variety of aliphatic (Scheme 4) and aromatic (Scheme 5) aldehydes were tested. The desired

**SCHEME 4** | Substrate scope—aliphatic aldehydes.**SCHEME 5** | Substrate scope—aromatic aldehydes.

products **4a–4j** were obtained in good to excellent yields, even in the case of α,α -disubstituted aldehydes (**4e–4g**). In an effort to expand our method's application, aldehydes bearing a large aliphatic chain, double or triple bond were tested, leading to the desired products **4h–4j** in good yields (65%–78%). In the case of aromatic aldehydes, we initially tested some substrates (**4k–4q**) using procedure **A** (2.5 equiv. MeOH in 1 mL Pet. eth.). However, we observed that the yields were moderate (44%–61%), with *para*-nitro-benzaldehyde not producing any product, as shown in Scheme 5. Thus, we developed procedure **B** (1 mL MeOH) for all aromatic aldehydes, without compromising the



SCHEME 6 | Substrate scope—alcohols.

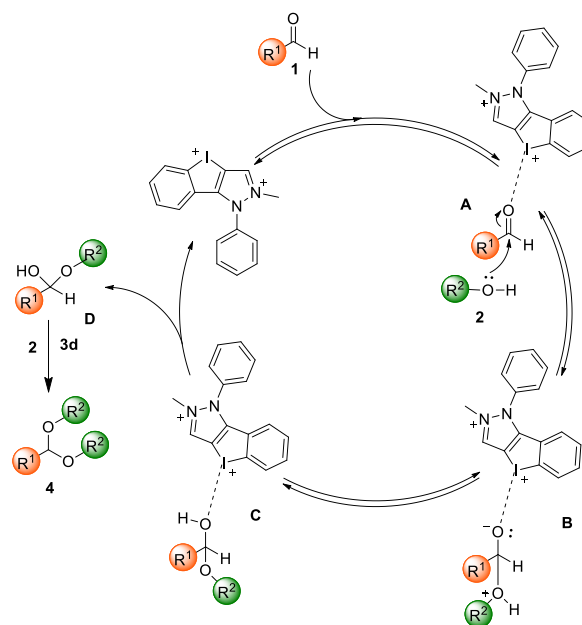
methodology, since *para*-, *meta*- or *ortho*-substituted aromatic aldehydes afforded yields that varied from 24% to 97%. Also, naphthaldehyde (**4w**) and heteroaromatic furfuryl aldehyde (**4x**) led to the desired product in 74% and 69% yield, respectively.

Subsequently, we explored the scope of alcohols utilizing **1a** as the starting material, providing the desired acetals in good to excellent yields (Scheme 6). Primary alcohols and alcohols bearing functional groups, such as a chloride group were utilized successfully, leading to the desired acetals in good yields (55%–80%). Secondary alcohols, alcohols bearing functional groups, such as $-\text{CF}_3$ group, or diols were tested successfully with procedure **B** and the products were obtained in 30%–55% yield.

A proposed mechanism for this protocol is shown in Scheme 7. Iodonium catalyst **3d** can enhance the electrophilicity of aldehyde **1**, through XB, leading to complex **A** (Scheme 7). This is in accordance with the observations of our previous mechanistic studies using NMR between **1a** and **3e** [75]. This complexation facilitates nucleophilic addition of the alcohol, affording tetrahedral intermediate **B**. This intermediate can then collapse, regenerating the organocatalyst and forming hemiacetal intermediate **D**. This can react with another molecule of alcohol, to afford the desired product **4**.

3 | Conclusion

In conclusion, a mild and efficient organocatalytic protocol was developed, activating aldehydes for their reaction with alcohols, leading to acetals. This method relies on a small organic molecule activating efficiently both aliphatic and aromatic aldehydes via XB, leading to acetals in good to high yields. Although, a straightforward linear correlation between calculated and experimental data is not evident, this study demonstrates that the relative catalytic efficiency can be reliably predicted by evaluating key energetic and geometric parameters across the catalyst series. While the intermediate catalysts (**3c** and **3e**) cannot be distinctly



SCHEME 7 | Proposed reaction mechanism. The anions are omitted for better clarity.

separated in terms of performance based solely on these descriptors, the extremes of the catalytic activity range—the most and least effective catalysts—are well predicted by the computational metrics.

4 | Experimental Section

General Procedure for the Organocatalytic Reaction Between Aliphatic Aldehydes and Alcohols

General Procedure A: In a glass vial, catalyst **3d** (7.0 mg, 0.01 mmol), aldehyde (0.50 mmol), and alcohol (1.25 mmol) were added consecutively in petroleum ether (1 mL). The vial was left stirring for 18 h. The desired product was isolated after purification by column chromatography.

General Procedure B: In a glass vial, catalyst **3d** (7.0 mg, 0.01 mmol) and aldehyde (0.50 mmol) were added consecutively in alcohol (1 mL). The vial was left stirring for 18 h. The desired product was isolated after purification by column chromatography.

Supporting Information

The authors have cited additional references within the Supporting Information [86, 87, 95–98, 114–125].

Acknowledgments

The authors gratefully acknowledge the Hellenic Foundation for Research and Innovation (HFRI) for financial support through a grant, which is financed by the first Call for H.F.R.I. Research Projects to Support Faculty Members & Researchers and a procurement of high-cost research equipment grant (grant number 655). Part of this work was carried out

as part of the “Industrial PhD Program” under the National Recovery and Resilience Plan “Greece 2.0”, specifically within the framework of the Reform “Enhancing Quality, Innovation, and Extroversion in Universities” (grant number YΠΠΑ-0559149).

The publication of this article in OA mode was financially supported by HEAL-Link.

Conflicts of Interest

The authors declare no conflicts of interest.

Data Availability Statement

The data that support the findings of this study are available in the supplementary material of this article.

References

1. P. S. Baran and J. M. Richter, “Direct Coupling of Indoles With Carbonyl Compounds: Short, Enantioselective, Gram-Scale Synthetic Entry Into the Hapalindole and Fischerindole Alkaloid Families,” *Journal of the American Chemical Society* 126 (2004): 7450–7451, <https://doi.org/10.1021/ja047874w>.
2. S. Krautwald, D. Sarlah, M. A. Schafröth, and E. M. Carreira, “Enantio- and Diastereodivergent Dual Catalysis: α -Allylation of Branched Aldehydes,” *Science* 340 (2013): 1065–1068, <https://doi.org/10.1126/science.1237068>.
3. T. Sandmeier, S. Krautwald, H. F. Zipfel, and E. M. Carreira, “Stereodivergent Dual Catalytic α -Allylation of Protected α -Amino- and α -Hydroxyacetaldehydes,” *Angewandte Chemie International Edition* 54 (2015): 14363–14367, <https://doi.org/10.1002/anie.201506933>.
4. L. R. Malins, J. N. deGruyter, and K. J. Robbins, “Peptide Macrocyclization Inspired by Non-Ribosomal Imine Natural Products,” *Journal of the American Chemical Society* 139 (2017): 5233–5241, <https://doi.org/10.1021/jacs.7b01624>.
5. D. M. Clode, “Carbohydrate Cyclic Acetal Formation and Migration,” *Chemical Reviews* 79 (1979): 491–513, <https://doi.org/10.1021/cr60322a002>.
6. K. Bauer, D. Garbe, and H. Surburg *Common Fragrances and Flavor Materials: Preparation and Uses* 5th edition (2001): 103–110.
7. P. G. M. Wuts and T. W. Greene, *Greene’s Protective Groups in Organic Synthesis* 4th edition (2007): 424–428.
8. P. A. Bartlett, W. S. Johnson, and J. D. Elliott, “Asymmetric Synthesis via Acetal Templates. 3. On the Stereochemistry Observed in the Cyclization of Chiral Acetals of Polyolefinic Aldehydes; Formation of Optically Active Homoallylic Alcohols,” *Journal of the American Chemical Society* 105 (1983): 2088–2089, <https://doi.org/10.1021/ja00345a082>.
9. A. Mori and H. Yamamoto, “Resolution of Ketones via Chiral Acetals. Kinetic Approach,” *Journal of Organic Chemistry* 50 (1985): 5444–5446, <https://doi.org/10.1021/jo00225a108>.
10. T. Xu, Z. Yu, and L. Wang, “Iron-Promoted Cyclization/Halogenation of Alkynyl Diethyl Acetals,” *Organic Letters* 11 (2009): 2113–2116, <https://doi.org/10.1021/ol9005689>.
11. Z.-B. Zhu, Y. Wie, and M. Shi, “Acid-Catalyzed Cascade Reactions of Arylvinylicyclopropenes With Acetals and Aldehydes for the Construction of Different Aromatic Systems,” *Chemistry—A European Journal* 15 (2009): 7543–7548, <https://doi.org/10.1002/chem.200900948>.
12. I. Suzuki, M. Yasuda, and A. Baba, “Zn(II) Chloride-Catalyzed Direct Coupling of Various Alkynes With Acetals: Facile and Inexpensive Access to Functionalized Propargyl Ethers,” *Chemical Communications* 49 (2013): 11620–11622, <https://doi.org/10.1039/c3cc46570e>.
13. Q. Yang, T. Xu, and Z. Yu, “Iron-Mediated Carboarylation/Cyclization of Propargylanilines With Acetals: A Concise Route to Indeno[2,1-c]Quinolines,” *Organic Letters* 16 (2014): 6310–6313, <https://doi.org/10.1021/ol503039j>.
14. H. Maarse, *Volatile Compounds I Foods and Beverages*, Marcel Dekker (New York, 1991).
15. P. H. R. Silva, V. L. C. Gonçalves, and C. J. A. Mota, “Glycerol Acetals as Anti-Freezing Additives for Biodiesel,” *Bioresource Technology* 101 (2010): 6225–6229, <https://doi.org/10.1016/j.biortech.2010.02.101>.
16. T. H. Fife and L. K. Jao, “Substituent Effects in Acetal Hydrolysis,” *Journal of Organic Chemistry* 30 (1965): 1492–1495, <https://doi.org/10.1021/jo01016a036>.
17. S. Sugai, T. Kodama, S. Akaboshi, and S. Ikegami, “A Simple and Efficient Conversion of Aldehyde Acetals Into Esters,” *Chemical and Pharmaceutical Bulletin* 32 (1984): 99–105, <https://doi.org/10.1248/cpb.32.99>.
18. R. A. Ugarte and T. W. Hudnall, “Antimony(V) Catalyzed Acetalisation of Aldehydes: An Efficient, Solvent-Free, and Recyclable Process,” *Green Chemistry* 19 (2017): 1990–1998, <https://doi.org/10.1039/C6GC03629E>.
19. S. A. Patwardhan and S. Der, “Amberlyst-15, a Superior Catalyst for the Preparation of Enol Ethers and Acetals,” *Synthesis* 1974 (1974): 348–349, <https://doi.org/10.1055/s-1974-23314>.
20. L. Myles, R. Gore, M. Špulák, N. Gathergood, and S. J. Connon, “Highly Recyclable, Imidazolium Derived Ionic Liquids of Low Antimicrobial and Antifungal Toxicity: A New Strategy for Acid Catalysis,” *Green Chemistry* 12 (2010): 1157–1162, <https://doi.org/10.1039/c003301d>.
21. M. X. Tan, L. Gu, N. Li, J. Y. Ying, and Y. Zhang, “Mesoporous Poly-Melamine-Formaldehyde (mPMF)—A Highly Efficient Catalyst for Chemoselective Acetalization of Aldehydes,” *Green Chemistry* 15 (2013): 1127–1132, <https://doi.org/10.1039/c3gc40297e>.
22. D. B. G. Williams and M. C. Lawton, “Highly Atom Efficient Aluminium Triflate Catalysed Acetal Formation,” *Green Chemistry* 10 (2008): 914–917, <https://doi.org/10.1039/b805748f>.
23. Z. Miao, L. Xu, H. Song, H. Zhao, and L. Chou, “One-Pot Synthesis of Ordered Mesoporous Zirconium Oxophosphate With High Thermostability and Acidic Properties,” *Catalysis Science & Technology* 3 (2013): 1942–1954, <https://doi.org/10.1039/c3cy00085k>.
24. N. M. Leonard, M. C. Oswald, D. A. Freiberg, B. A. Nattier, R. C. Smith, and R. S. Mohan, “A Simple and Versatile Method for the Synthesis of Acetals From Aldehydes and Ketones Using Bismuth Triflate,” *Journal of Organic Chemistry* 67 (2002): 5202–5207, <https://doi.org/10.1021/jo0258249>.
25. S. M. Patel, U. V. Chudasama, and P. A. Ganeshpure, “Ketalization of Ketones With Diols Catalyzed by Metal(IV) Phosphates as Solid Acid Catalysts,” *Journal of Molecular Catalysis A: Chemical* 194 (2003): 267–271, [https://doi.org/10.1016/S1381-1169\(02\)00538-1](https://doi.org/10.1016/S1381-1169(02)00538-1).
26. J.-Y. Qi, J.-X. Ji, C.-H. Yueng, H.-L. Kwong, and A. S. C. Chan, “A Convenient and Highly Efficient Method for the Protection of Aldehydes Using Very Low Loading Hydrous Ruthenium(III) Trichloride as Catalyst,” *Tetrahedron Letters* 45 (2004): 7719–7721, <https://doi.org/10.1016/j.tetlet.2004.08.112>.
27. R. Kumar and A. K. Chakraborti, “Copper(II) Tetrafluoroborate as a Novel and Highly Efficient Catalyst for Acetal Formation,” *Tetrahedron Letters* 46 (2005): 8319–8323, <https://doi.org/10.1016/j.tetlet.2005.09.168>.
28. H. Mansilla and M. M. Afonso, “Iron(III) Tosylate in the Preparation of Dimethyl and Diethyl Acetals From Ketones and β -Keto Enol Ethers From Cyclic β -Diketones,” *Synthetic Communications* 38 (2008): 2607–2618, <https://doi.org/10.1080/00397910802219361>.
29. A. D. Chowdhury and G. K. Lahiri, “A Generalized Approach for Iron Catalyzed Chemo- and Regioselective Formation of Anti-Markovnikov Acetals From Styrene Derivatives,” *Chemical Communications* 48 (2012): 3448–3450, <https://doi.org/10.1039/c2cc17889c>.
30. A. Thurkauf, A. E. Jacobson, and K. C. Riee, “An Improved Procedure for the Preparation of Acetals From Diaryl Ketones,” *Synthesis* 1988 (1988): 233–234, <https://doi.org/10.1055/s-1988-27525>.
31. B. Procuranti and S. J. Connon, “Unexpected Catalysis: Aprotic Pyridinium Ions as Active and Recyclable Brønsted Acid Catalysts in

- Protic media," *Organic Letters* 10 (2008): 4935–4938, <https://doi.org/10.1021/ol802008m>.
32. A. J. Showler and P. A. Darley, "Condensation Products of Glycerol With Aldehydes and Ketones. 2-Substituted M-Dioxan-5-ols and 1,3-Dioxolane-4-methanols," *Chemical Reviews* 67 (1967): 427–440, <https://doi.org/10.1021/cr60248a003>.
33. P. T. Anastas and J. C. Warner, *Green Chemistry: Theory and Practice* (University Press, 1998).
34. J. Grabowski, J. M. Granda, and J. Jurczak, "Preparation of Acetals From Aldehydes and Alcohols Under Basic Conditions," *Organic & Biomolecular Chemistry* 16 (2018): 3114–3120, <https://doi.org/10.1039/C8OB00017D>.
35. K. J. Mickelsen, C. M. Tajc, K. R. Greenwood, and C. C. Browder, "Method for the Selective Formation of Dimethyl Acetals in the Presence of Hydroxylamine," *Synthetic Communications* 42 (2012): 186–194, <https://doi.org/10.1080/00397911.2010.523156>.
36. M. K. Basu, S. Samajdar, F. F. Becker, and B. K. Banik, "A New Molecular Iodine-Catalyzed Acetalization of Carbonyl Compounds," *Synlett* 2002 (2002): 0319–0321, <https://doi.org/10.1055/s-2002-19774>.
37. B. Karimi and B. Golshani, "Iodine-Catalyzed, Efficient and Mild Procedure for Highly Chemoselective Acetalization of Carbonyl Compounds Under Neutral Aprotic Conditions," *Synthesis* 2002 (2002): 784–788, <https://doi.org/10.1055/s-2002-25775>.
38. K. Kumamoto, Y. Ichikawa, and H. Kotsuki, "High-Pressure-Promoted Uncatalyzed Ketalization of Ketones and Oxy-Michael/Ketalization of Conjugated Enones [1]," *Synlett* 14 (2005): 2254–2256.
39. M. Barbasiewicz and M. Małozosza, "Intermolecular Reactions of Chlorohydrine Anions: Acetalization of Carbonyl Compounds Under Basic Conditions," *Organic Letters* 8 (2006): 3745–3748, <https://doi.org/10.1021/ol0613113>.
40. S. Zhao, Y. Jia, and Y. F. Song, "Acetalization of Aldehydes and Ketones over H₄[SiW₁₂O₄₀] and H₄[SiW₁₂O₄₀]/SiO₂," *Catalysis Science & Technology* 4 (2014): 2618–2625, <https://doi.org/10.1039/C4CY00021H>.
41. M. D. Kärkäs, J. A. Porco, and C. R. J. Stephenson, "Photochemical Approaches to Complex Chemotypes: Applications in Natural Product Synthesis," *Chemical Reviews* 116 (2016): 9683–9747, <https://doi.org/10.1021/acs.chemrev.5b00760>.
42. K. L. Scubi, T. R. Blum, and T. P. Yoon, "Dual Catalysis Strategies in Photochemical Synthesis," *Chemical Reviews* 116 (2016): 10035–10074, <https://doi.org/10.1021/acs.chemrev.6b00018>.
43. N. A. Romero and D. A. Nicewicz, "Organic Photoredox Catalysis," *Chemical Reviews* 116 (2016): 10075–10166, <https://doi.org/10.1021/acs.chemrev.6b00057>.
44. D. Cambie, C. Bottecchia, N. J. W. Straathof, V. Hessel, and T. Noel, "Applications of Continuous-Flow Photochemistry in Organic Synthesis, Material Science, and Water Treatment," *Chemical Reviews* 116 (2016): 10276–10341, <https://doi.org/10.1021/acs.chemrev.5b00707>.
45. J. Schwarz and B. König, "Decarboxylative Reactions With and Without Light—A Comparison," *Green Chemistry* 20 (2018): 323–361, <https://doi.org/10.1039/C7GC02949G>.
46. P. L. Gkizis, I. Triandafillidi, and C. G. Kokotos, "Nitroarenes: The Rediscovery of Their Photochemistry Opens New Avenues in Organic Synthesis," *Chem* 9 (2023): 3401–3414, <https://doi.org/10.1016/j.chempr.2023.09.008>.
47. V. P. Demertzidou, E. Skolia, and C. G. Kokotos, "Thioxanthone: A Benchmark Photocatalyst for Organic Synthesis," *ChemCatChem* 17 (2025): e00760, <https://doi.org/10.1002/cctc.202500760>.
48. H. Yi, L. Niu, S. Wang, T. Liu, A. K. Singh, and A. Lei, "Visible-Light-Induced Acetalization of Aldehydes With Alcohols," *Organic Letters* 19 (2017): 122–125, <https://doi.org/10.1021/acs.orglett.6b03403>.
49. I. Triandafillidi, M. G. Kokotou, and C. G. Kokotos, "Photocatalytic Synthesis of γ -Lactones From Alkenes: High-Resolution Mass Spectrometry as a Tool To Study Photoredox Reactions," *Organic Letters* 20 (2018): 36–39, <https://doi.org/10.1021/acs.orglett.7b03256>.
50. N. F. Nikitas, D. I. Tzaras, I. Triandafillidi, and C. G. Kokotos, "Photochemical Oxidation of Benzylic Primary and Secondary Alcohols Utilizing Air as the Oxidant," *Green Chemistry* 22 (2020): 471–477, <https://doi.org/10.1039/C9GC03000J>.
51. E. Voutyritsa and C. G. Kokotos, "Green Metal-Free Photochemical Hydroacylation of Unactivated Olefins," *Angewandte Chemie International Edition* 59 (2020): 1735–1741, <https://doi.org/10.1002/anie.201912214>.
52. N. F. Nikitas, M. K. Apostolopoulou, E. Skolia, A. Tsoukaki, and C. G. Kokotos, "Photochemical Activation of Aromatic Aldehydes: Synthesis of Amides, Hydroxamic Acids and Esters," *Chemistry—A European Journal* 27 (2021): 7915–7922, <https://doi.org/10.1002/chem.202100655>.
53. E. M. Galathri, L. Di Terlizzi, M. Fagnoni, S. Protti, and C. G. Kokotos, "Friedel–Crafts Arylation of Aldehydes With Indoles Utilizing Arylazo Sulfones as the Photoacid Generator," *Organic & Biomolecular Chemistry* 21 (2023): 365–369, <https://doi.org/10.1039/D2OB02214A>.
54. P. X. Kolagkis, E. M. Galathri, and C. G. Kokotos, "Light-Driven Michael Addition of Indoles to β -Nitroolefins in Aqueous Medium," *Catalysis Today* 441 (2024): 114868, <https://doi.org/10.1016/j.cattod.2024.114868>.
55. E. M. Galathri, L. Di Terlizzi, M. Fagnoni, S. Protti, and C. G. Kokotos, "Photochemical Michael Addition of Indoles to α,β -Unsaturated Ketones utilizing Arylazo Sulfones as the Photoacid Generators," *ChemCatChem* 16 (2024): e202400686.
56. E. Skolia, O. G. Mountanea, and C. G. Kokotos, "Photochemical Aerobic Upcycling of Polystyrene Plastics," *ChemSusChem* 17 (2024): e202400174.
57. N. A. Stini, P. L. Gkizis, I. Triandafillidi, and C. G. Kokotos, "Photocatalytic CeCl₃-Promoted C-H Alkenylation and Alkynylation of Alkanes," *Chemistry - A European Journal* 31 (2025): e202404063.
58. G. Michael, P. X. Kolagkis, E. M. Galathri, and C. G. Kokotos, "Photoorganocatalytic Hydroacylation of Unactivated Olefins Utilizing Naphthaloylidenebenzimidazole (NBI) as the Catalyst," *Synlett* 36 (2025): 1559–1564.
59. N. F. Nikitas, I. Triandafillidi, and C. G. Kokotos, "Photo-Organocatalytic Synthesis of Acetals From Aldehydes," *Green Chemistry* 21 (2019): 669–674, <https://doi.org/10.1039/C8GC03605E>.
60. N. Spiliopoulou, N. F. Nikitas, and C. G. Kokotos, "Photochemical Synthesis of Acetals Utilizing Schreiner's Thiourea as the Catalyst," *Green Chemistry* 22 (2020): 3539–3545, <https://doi.org/10.1039/D0GC01135E>.
61. J. Saway, A. F. Pierre, and J. J. Badillo, "Photoacid-Catalyzed Acetalization of Carbonyls With Alcohols," *Organic & Biomolecular Chemistry* 20 (2022): 6188–6192, <https://doi.org/10.1039/D2OB00435F>.
62. D. Arnodo, C. Meazzo, S. Baldino, M. Blangetti, and C. Prandi, "Efficient and Low-Impact Acetalization Reactions in Deep Eutectic Solvents," *Chemistry: A European Journal* 29 (2023): e202300820.
63. S. Mondal, D. Manna, and G. Mughesh, "Selenium-Mediated Dehalogenation of Halogenated Nucleosides and Its Relevance to the DNA Repair Pathway," *Angewandte Chemie International Edition* 54 (2015): 9298–9302, <https://doi.org/10.1002/anie.201503598>.
64. G. Cavallo, P. Metrangolo, R. Milani, T. Pilati, A. Priimagi, G. Resnati, and G. Terraneo, "The Halogen Bond," *Chemical Reviews* 116 (2016): 2478–2601, <https://doi.org/10.1021/acs.chemrev.5b00484>.
65. S. K. Mahapatra, B. Ghosh, and L. Roy, "Harnessing Selectivity and Reactivity with Noncovalent Interactions in Molecular and Supramolecular Organo-Catalysis: A Computational Perspective," *ChemCatChem* 17 (2025): e01069.
66. A. Mukherjee, S. Tothadi, and G. R. Desiraju, "Halogen Bonds in Crystal Engineering: Like Hydrogen Bonds yet Different," *Accounts of Chemical Research* 47 (2014): 2514–2524, <https://doi.org/10.1021/ar5001555>.

67. M. S. Taylor, "Anion Recognition Based on Halogen, Chalcogen, Pnictogen and Tetrel Bonding," *Coordination Chemistry Reviews* 413 (2020): 213270, <https://doi.org/10.1016/j.ccr.2020.213270>.
68. D. Bulfield and S. M. Huber, "Halogen Bonding in Organic Synthesis and Organocatalysis," *Chemistry—A European Journal* 22 (2016): 14434–14450, <https://doi.org/10.1002/chem.201601844>.
69. A. Bauza, T. J. Mooibroek, and A. Frontera, "The Bright Future of Unconventional σ/π -Hole Interactions," *ChemPhysChem* 16 (2015): 2496–2517, <https://doi.org/10.1002/cphc.201500314>.
70. M. Breugst and J. J. Koenig, " σ -Hole Interactions in Catalysis," *European Journal of Organic Chemistry* 2020 (2020): 5473–5487, <https://doi.org/10.1002/ejoc.202000660>.
71. J. Bamberger, F. Ostler, and O. G. Mancheno, "Frontiers in Halogen and Chalcogen-Bond Donor Organocatalysis," *ChemCatChem* 11 (2019): 5198–5211, <https://doi.org/10.1002/cctc.201901215>.
72. O. G. Mountanea, D. Psathopoulou, C. Mantzourani, et al., "An Efficient Light-Mediated Protocol for the Direct Amide Bond Formation via a Novel Carboxylic Acid Photoactivation Mode by Pyridine-CBr₄," *Chemistry: A European Journal* 29 (2023): e202300556.
73. A. Bourboula, O. G. Mountanea, G. Krasakis, et al., "A Photochemical Protocol for the Synthesis of Weinreb and Morpholine Amides from Carboxylic Acids," *European Journal of Organic Chemistry* 26 (2023): e202300008.
74. O. G. Mountanea, C. Mantzourani, M. G. Kokotou, C. G. Kokotos, and G. Kokotos, "Sunlight- or UVA-Light-Mediated Synthesis of Hydroxamic Acids from Carboxylic Acids," *European Journal of Organic Chemistry* 26 (2023): e202300046.
75. E. M. Galathri, T. J. Kuczmera, B. J. Nachtsheim, and C. G. Kokotos, "Organocatalytic Friedel–Crafts Arylation of Aldehydes With Indoles Utilizing N-Heterocyclic Iod(az)Olium Salts as Halogen-Bonding Catalysts," *Green Chemistry* 26 (2024): 825–831, <https://doi.org/10.1039/D3GC03687A>.
76. R. L. Sutar and S. M. Huber, "Catalysis of Organic Reactions through Halogen Bonding," *ACS Catalysis* 9 (2019): 9622–9639, <https://doi.org/10.1021/acscatal.9b02894>.
77. H. Yang and M. W. Wong, "Application of Halogen Bonding to Organocatalysis: A Theoretical Perspective," *Molecules (Basel, Switzerland)* 25 (2020): 1045, <https://doi.org/10.3390/molecules25051045>.
78. C. Bolm, A. Bruckmann, and M. Pena, "Organocatalysis through Halogen-Bond Activation," *Synlett* 2008 (2008): 900–902, <https://doi.org/10.1055/s-2008-1042935>.
79. A. Boelke, E. Lork, and B. J. Nachtsheim, "N-Heterocycle-Stabilized Iodanes: From Structure to Reactivity," *Chemistry—A European Journal* 24 (2018): 18653–18657, <https://doi.org/10.1002/chem.201804957>.
80. A. Boelke, Y. A. Vlasenko, M. S. Yusubov, B. J. Nachtsheim, and P. S. Postnikov, "Thermal Stability of N-Heterocycle-Stabilized Iodanes—A Systematic Investigation," *Beilstein Journal of Organic Chemistry* 15 (2019): 2311–2318, <https://doi.org/10.3762/bjoc.15.223>.
81. A. Boelke, T. J. Kuczmera, L. D. Caspers, E. Lork, and B. J. Nachtsheim, "Iodolopyrazolium Salts: Synthesis, Derivatizations, and Applications," *Organic Letters* 22 (2020): 7261–7266, <https://doi.org/10.1021/acs.orglett.0c02593>.
82. A. Boelke and B. J. Nachtsheim, "Evolution of N-Heterocycle-Substituted Iodoarenes (NHIA)s to Efficient Organocatalysts in Iodine(I/III)-Mediated Oxidative Transformations," *Advanced Synthesis & Catalysis* 362 (2020): 184–191, <https://doi.org/10.1002/adsc.201901356>.
83. A. H. Abazid and B. J. Nachtsheim, "A Triazole-Substituted Aryl Iodide With Omnipotent Reactivity in Enantioselective Oxidations," *Angewandte Chemie International Edition* 59 (2020): 1479–1484, <https://doi.org/10.1002/anie.201912023>.
84. A. H. Abazid, N. Clamor, and B. J. Nachtsheim, "An Enantioconvergent Benzylic Hydroxylation Using a Chiral Aryl Iodide in a Dual Activation Mode," *ACS Catalysis* 10 (2020): 8042–8048, <https://doi.org/10.1021/acscatal.0c02321>.
85. A. Boelke, T. J. Kuczmera, E. Lork, and B. J. Nachtsheim, "N-Heterocyclic Iod(az)Olium Salts—Potent Halogen-Bond Donors in Organocatalysis," *Chemistry—A European Journal* 27 (2021): 13128–13134, <https://doi.org/10.1002/chem.202101961>.
86. P. Pracht, F. Bohle, and S. Grimme, "Automated Exploration of the Low-Energy Chemical Space With Fast Quantum Chemical Methods," *Physical Chemistry Chemical Physics* 22 (2020): 7169–7192, <https://doi.org/10.1039/C9CP06869D>.
87. P. Pracht, S. Grimme, and C. Bannwarth, "CREST—A Program for the Exploration of Low-Energy Molecular Chemical Space," *Journal of Chemical Physics* 160 (2024): 114110, <https://doi.org/10.1063/5.0197592>.
88. F. Neese, "Approximate Second-Order SCF Convergence for Spin Unrestricted Wavefunctions," *Chemical Physics Letters* 325 (2000): 93–98, [https://doi.org/10.1016/S0009-2614\(00\)00662-X](https://doi.org/10.1016/S0009-2614(00)00662-X).
89. F. Neese, "An Improvement of the Resolution of the Identity Approximation for the Formation of the Coulomb Matrix," *Journal of Computational Chemistry* 24 (2003): 1740–1747, <https://doi.org/10.1002/jcc.10318>.
90. F. Neese, "The ORCA Program System," *WIREs Computational Molecular Science* 2 (2012): 73–78, <https://doi.org/10.1002/wcms.81>.
91. F. Neese, "Efficient and Accurate Approximations to the Molecular Spin-Orbit Coupling Operator and Their use in Molecular-Tensor Calculations," *Journal of Computational Chemistry* 44 (2022): 1–16.
92. F. Neese, F. Wennmohs, U. Becker, and C. Riplinger, "The ORCA Quantum Chemistry Program Package," *Journal of Chemical Physics* 152 (2020): 224108, <https://doi.org/10.1063/5.0004608>.
93. F. Neese, F. Wennmohs, A. Hansen, and U. Becker, "Efficient, Approximate and Parallel Hartree–Fock and Hybrid DFT Calculations. A 'Chain-of-Spheres' Algorithm for the Hartree–Fock Exchange," *Chemical Physics* 356 (2009): 98–109, <https://doi.org/10.1016/j.chemphys.2008.10.036>.
94. S. K. Mahapatra, B. Ghosh, and L. Roy, "Harnessing Selectivity and Reactivity With Noncovalent Interactions in Molecular and Supramolecular Organo-Catalysis: A Computational Perspective," *ChemCatChem* 17 (2025): e01069, <https://doi.org/10.1002/cctc.202501069>.
95. A. D. Becke, "Density-Functional Thermochemistry. III. The Role of Exact Exchange," *Journal of Chemical Physics* 98 (1993): 5648–5652, <https://doi.org/10.1063/1.464913>.
96. C. Lee, W. Yang, and R. G. Parr, "Development of the Colle-Salvetti Correlation-Energy Formula Into a Functional of the Electron Density," *Physical Review B* 37 (1988): 785–789, <https://doi.org/10.1103/PhysRevB.37.785>.
97. S. H. Vosko, L. Wilk, and M. Nusair, "Accurate Spin-Dependent Electron Liquid Correlation Energies for Local Spin Density Calculations: A Critical Analysis," *Canadian Journal of Physics* 58 (1980): 1200–1211, <https://doi.org/10.1139/p80-159>.
98. P. J. Stephens, F. J. Devlin, C. F. Chabalowski, and M. J. Frisch, "Ab Initio Calculation of Vibrational Absorption and Circular Dichroism Spectra Using Density Functional Force Fields," *Journal of Physical Chemistry* 98 (1994): 11623–11627, <https://doi.org/10.1021/j100096a001>.
99. F. Weigend and R. Ahlrichs, "Balanced Basis Sets of Split Valence, Triple Zeta Valence and Quadruple Zeta Valence Quality for H to Rn: Design and Assessment of Accuracy," *Physical Chemistry Chemical Physics* 7 (2005): 3297–3305, <https://doi.org/10.1039/b508541a>.
100. S. Grimme, J. Antony, S. Ehrlich, and H. Krieg, "A Consistent and Accurate Ab Initio Parametrization of Density Functional Dispersion Correction (DFT-D) for the 94 Elements H–Pu," *Journal of Chemical Physics* 132 (2010): 154104, <https://doi.org/10.1063/1.3382344>.
101. Y.-S. Lin, G.-D. Li, S.-P. Mao, and J.-D. Chai, "Long-Range Corrected Hybrid Density Functionals With Improved Dispersion Corrections," *Journal of Chemical Theory and Computation* 9 (2013): 263–272, <https://doi.org/10.1021/ct300715s>.

102. E. Caldeweyher, S. Ehlert, and A. Hansen, "A Generally Applicable Atomic-Charge Dependent London Dispersion Correction," *Journal of Chemical Physics* 150 (2019): 154122, <https://doi.org/10.1063/1.5090222>.
103. J. Rezac, K. E. Riley, and P. Hobza, "Benchmark Calculations of Noncovalent Interactions of Halogenated Molecules," *Journal of Chemical Theory and Computation* 8 (2012): 4285–4292, <https://doi.org/10.1021/ct300647k>.
104. C. Plett, M. Stahn, M. Bursch, J.-M. Mewes, and S. Grimme, "Improving Quantum Chemical Solvation Models by Dynamic Radii Adjustment for Continuum Solvation (DRACO)," *Journal of Physical Chemistry Letters* 15 (2024): 2462–2469, <https://doi.org/10.1021/acs.jpcllett.3c03551>.
105. M. Garcia-Rates and F. Neese, "Effect of the Solute Cavity on the Solvation Energy and Its Derivatives Within the Framework of the Gaussian Charge Scheme," *Journal of Computational Chemistry* 41 (2020): 922–939, <https://doi.org/10.1002/jcc.26139>.
106. S. F. Boys and F. Bernardi, "The Calculation of Small Molecular Interactions by the Differences of Separate Total Energies. Some Procedures With Reduced Errors," *Molecular Physics* 19 (1970): 553–566, <https://doi.org/10.1080/00268977000101561>.
107. T. Lu and F. Chen, "Multiwfn: A Multifunctional Wavefunction Analyzer," *Journal of Computational Chemistry* 33 (2012): 580–592, <https://doi.org/10.1002/jcc.22885>.
108. E. C. Meng, T. D. Goddard, and E. F. Pettersen, "UCSF ChimeraX: Tools for Structure Building and Analysis," *Protein Science* 32 (2023): e4792, <https://doi.org/10.1002/pro.4792>.
109. P. Politzer, J. S. Murray, T. Clark, and G. Resnati, "The σ -Hole Revisited," *Physical Chemistry Chemical Physics* 19 (2017): 32166–32178, <https://doi.org/10.1039/C7CP06793C>.
110. C. Zhao, Y. Li, X. Li, and Y. Zeng, "Iodine(i)-Based and Iodine(iii)-Based Halogen Bond Catalysis on the Friedel–Crafts Reaction: A Theoretical Study," *Physical Chemistry Chemical Physics* 25 (2023): 21100–21108, <https://doi.org/10.1039/D3CP02541A>.
111. J. S. Murray and P. Politzer, "Molecular Electrostatic Potentials and Noncovalent Interactions," *Wiley Interdisciplinary Reviews: Computational Molecular Science* 7 (2017): e1326.
112. J. P. Reid and J. M. Goodman, "Goldilocks Catalysts: Computational Insights Into the Role of the 3,3' Substituents on the Selectivity of BINOL-Derived Phosphoric Acid Catalysts," *Journal of the American Chemical Society* 138 (2016): 7910–7917, <https://doi.org/10.1021/jacs.6b02825>.
113. B. J. Barron, W.-T. Wong, P. Chiu, and K. K. Hii, "Goldilocks Effect" of Water in Lewis–Brønsted Acid and Base Catalysis," *ACS Catalysis* 6 (2016): 4189–4194, <https://doi.org/10.1021/acscatal.6b00800>.
114. D. Wang, F.-R. Cao, G. Lu, J. Ren, and B.-B. Zeng, "Practical Acetalization and Transacetalization of Carbonyl Compounds Catalyzed by Recyclable PVP-I," *Tetrahedron* 92 (2021): 132250, <https://doi.org/10.1016/j.tet.2021.132250>.
115. Z. Huang, R. Guan, and M. Shanmugam, "Oxidative Cleavage of Alkenes by O₂ With a Non-Heme Manganese Catalyst," *Journal of the American Chemical Society* 143 (2021): 10005–10013, <https://doi.org/10.1021/jacs.1c05757>.
116. L. Myles, R. G. Gore, N. Gathergood, and S. J. Connon, "A New Generation of Aprotic yet Brønsted Acidic Imidazolium Salts: Low Toxicity, High Recyclability and Greatly Improved Activity," *Green Chemistry* 15 (2013): 2740–2746, <https://doi.org/10.1039/c3gc40975a>.
117. L. Gremaud and A. Alexaki, "Enantioselective Copper-Catalyzed Conjugate Addition of Trimethylaluminum to β,γ -Unsaturated α -Ketoesters," *Angewandte Chemie International Edition* 51 (2012): 794–797, <https://doi.org/10.1002/anie.201107324>.
118. F. Neese, "Software Update: the ORCA Program System, Version 4.0," *WIREs Computational Molecular Science* 8 (2018): e1327.
119. C. Bannwarth, S. Ehlert, and S. Grimme, "GFN2-xTB—An Accurate and Broadly Parametrized Self-Consistent Tight-Binding Quantum Chemical Method With Multipole Electrostatics and Density-Dependent Dispersion Contributions," *Journal of Chemical Theory and Computation* 15 (2019): 1652–1671, <https://doi.org/10.1021/acs.jctc.8b01176>.
120. S. Ehlert, M. Stahn, S. Spicher, and S. Grimme, "Robust and Efficient Implicit Solvation Model for Fast Semiempirical Methods," *Journal of Chemical Theory and Computation* 17 (2021): 4250–4261, <https://doi.org/10.1021/acs.jctc.1c00471>.
121. D. Andrae, U. Häußermann, M. Dolg, H. Stoll, and H. Preuß, "Energy-Adjusted ab Initio Pseudopotentials for the Second and Third Row Transition Elements," *Theoretica Chimica Acta* 77 (1990): 123–141, <https://doi.org/10.1007/BF0114537>.
122. A. V. Marenich, C. J. Cramer, and D. G. Truhlar, "Universal Solvation Model Based on Solute Electron Density and on a Continuum Model of the Solvent Defined by the Bulk Dielectric Constant and Atomic Surface Tensions," *Journal of Physical Chemistry B* 113 (2009): 6378–6396, <https://doi.org/10.1021/jp810292n>.
123. J.-D. Chai and M. Head-Gordon, "Long-Range Corrected Hybrid Density Functionals With Damped Atom–Atom Dispersion Corrections," *Physical Chemistry Chemical Physics* 10 (2008): 6615–6620, <https://doi.org/10.1039/b810189b>.
124. T. Lu and Q. Chen, "Independent Gradient Model Based on Hirshfeld Partition: A New Method for Visual Study of Interactions in Chemical Systems," *Journal of Computational Chemistry* 43 (2022): 539–555, <https://doi.org/10.1002/jcc.26812>.
125. G. Zhurko and D. Zhurko Chemcraft Graphical Program for Visualization of Computed Results (2015), <https://www.chemcraftprog.com>.

Supporting Information

Additional supporting information can be found online in the Supporting Information section.

Supporting File: cctc70516-sup-0001-SuppMat.pdf.